Journal of Medicinal Chemistry

Article

pubs.acs.org/jmc

Automated Protein–Ligand Interaction Screening by Mass Spectrometry

Hannah J. Maple,[†] Rachel A. Garlish,[‡] Laura Rigau-Roca,[†] John Porter,[‡] Ian Whitcombe,[‡] Christine E. Prosser,[‡] Jeff Kennedy,[‡] Alistair J. Henry,[‡] Richard J. Taylor,[‡] Matthew P. Crump,*[,†] and John Crosby*[,†]

[†]School of Chemistry, University of Bristol, Cantock's Close, Clifton, Bristol BS8 1TS, United Kingdom

[‡]UCB Pharma, 216 Bath Road, Slough, Berkshire SL1 4EN, United Kingdom

Supporting Information

ABSTRACT: Identifying protein–ligand binding interactions is a key step during early-stage drug discovery. Existing screening techniques are often associated with drawbacks such as low throughput, high sample consumption, and dynamic range limitations. The increasing use of fragment-based drug discovery (FBDD) demands that these techniques also detect very weak interactions (mM K_D values). This paper presents the development and validation of a fully automated screen by mass spectrometry, capable of detecting fragment binding into the millimolar K_D range. Low sample consumption, high throughput, and wide dynamic range make this a highly attractive, orthogonal approach. The method was applied to screen 157 compounds in 6 h against the anti-apoptotic protein target Bcl-x_L. Mass spectrometry results were validated using STD-NMR, HSQC-NMR, and ITC experiments. Agreement between techniques suggests that mass spectrometry offers a powerful, complementary approach for screening.

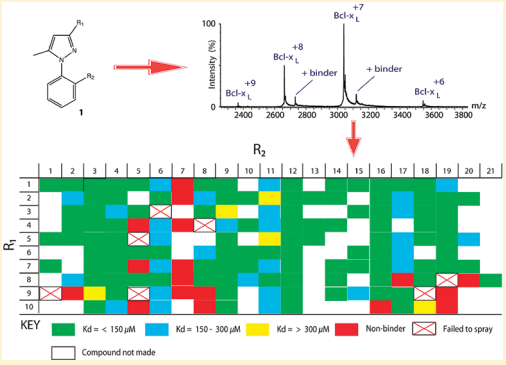

INTRODUCTION

The identification of chemical starting points in drug discovery is often a major bottleneck. High-throughput screening (HTS) hit rates are often low, and progression of hits is hampered by the difficulty associated with optimizing compounds while retaining drug-like properties.[1] Over the past decade, fragment-based drug discovery (FBDD) has emerged as an alternative approach for the generation of hit compounds against a protein target.[2] This method involves screening low molecular weight fragments (up to approximately 300 Da) instead of the larger molecules typically used in HTS campaigns. Due to their size, fragments have a higher ligand efficiency and improved chemical tractability. Fragment libraries can, therefore, explore greater chemical space within a protein binding site, which lowers the necessary library size for screening, and the corresponding hit rates are consequently higher than achieved with HTS. Fragments showing significant association with a target protein are then grown or chemically linked together with the aim of generating a selective binder. There are now a growing number of examples of the successful implementation of FBDD.[3,4]

The interactions of fragments with protein targets are limited, and they consequently bind weakly, with K_D values of the order of 100 μM–1 mM. Reliable detection of bound fragments therefore remains a challenge, although a variety of biophysical techniques have been successfully employed in the initial stages of FBDD, notably nuclear magnetic resonance (NMR),[5] surface plasmon resonance (SPR),[6] isothermal titration calorimetry (ITC),[7] and X-ray crystallography.[8] These methods are, however, all associated with at least one of the following drawbacks: high sample consumption, low throughput, dynamic range limitations, or the need to immobilize one of the binding partners. In addition, there is an inherent problem with reliability. Results from one technique do not always agree with those from an orthogonal method, and the occurrence of false positives and false negatives is common.[5]

Nanoelectrospray ionization mass spectrometry (nano-ESI MS) has emerged as a powerful technique for the detection and characterization of noncovalent interactions.[9] The strength of this technique lies with its inherent sensitivity (picomolar quantities of protein and ligand required), speed (as low as 30 s for each analysis), and ability to simultaneously determine binding stoichiometry and dissociation constants. This combination of factors confers significant advantages over other biophysical techniques used in FBDD. As with other experimental techniques, however, the reliability of biophysical parameters determined by nano-ESI MS has been questioned. There was initial skepticism that measurements conducted on proteins in the gas phase could accurately reflect structural characteristics in solution. This has been largely satisfied by

Received: October 8, 2011
Published: December 12, 2011

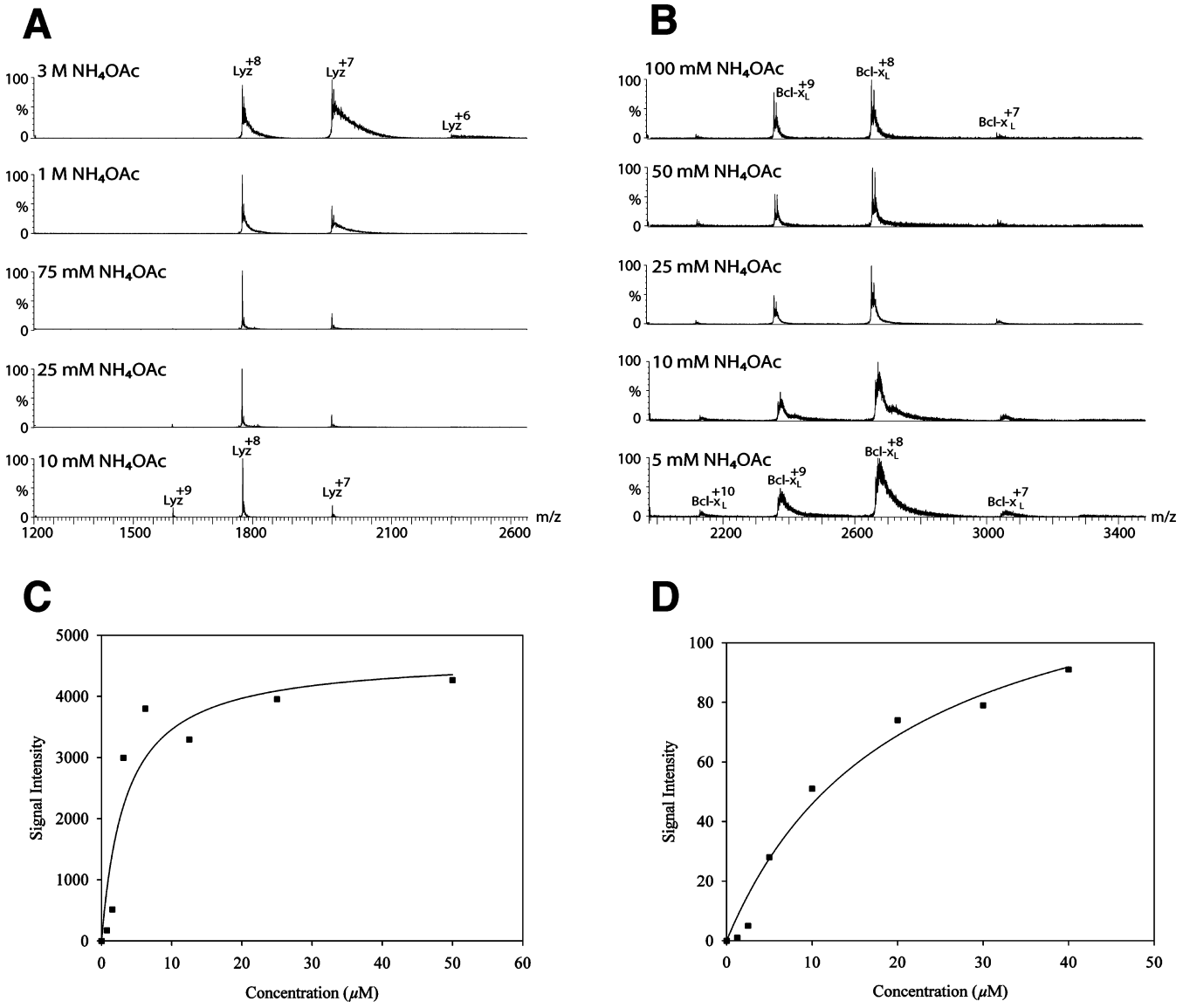

Figure 1. (A, B) Effect of ammonium acetate buffer concentration on the mass spectra of hen egg white lysozyme and Bcl-x_L, respectively. The protein concentration was 10 μM in both cases. (C, D) Effect of protein concentration on signal intensity for hen egg white lysozyme and Bcl-x_L, respectively.

substantial evidence that the native fold of proteins can be retained during the electrospray transfer to the gas phase.[10,11] Additionally, as solvent molecules are removed during the desolvation process, ionic and electrostatic interactions are strengthened, whereas hydrophobic and van der Waals forces are attenuated.[12] Relative strengths of the solution phase binding may therefore not be reflected in gas phase measurements,[13] and in some cases this may preclude detection of the complex.[14] There are, however, a number of papers detailing the detection of hydrophobically driven interactions in vacuo, which provide encouraging evidence that in some circumstances these complexes can be maintained intact during the electrospray process.[11,15,16] This may not be a major issue for fragment screening because hydrophobic interactions contribute mainly to the binding entropy. Improving ΔH for a protein−ligand interaction is significantly more problematic than optimizing ΔS, and enthalpic interactions are, therefore, sought preferentially in FBDD.[17] Weakening of entropically bound fragments in vacuo may bias the technique toward the more favorable enthalpically driven binders, and this differentiation has been suggested as an advantage of MS over other biophysical techniques.[18]

In this paper we discuss the practical considerations required to routinely detect ligand binding by nano-ESI MS. Data are presented on a test protein, hen egg white lysozyme, using a series of binders across a wide K_D range from low micromolar to millimolar. Under optimized conditions, K_D values generated by nano-ESI MS were in agreement with values obtained using solution phase techniques such as ITC. The subsequent development of a fully automated, high-throughput screen by nano-ESI MS is also presented, enabling rapid screening using only microgram quantities of protein and ligand. This extends the scope of previous studies in both sample size and the use of a TriVersa NanoMate (Advion) automation platform[19−22] and provides validation of a nano-ESI MS-based screening study that has been reported.[23] We have applied this method to screen a targeted library containing 157 compounds against an anti-apoptotic protein, Bcl-x_L, a member of the Bcl-2 family.[24]

dx.doi.org/10.1021/jm201347k | J. Med. Chem. 2012, 55, 837−851

Bcl-x_L is involved in the regulation of mitochondrion-mediated apoptosis within mammalian cells. Overexpression of this protein in many cancer cells is thought to play a role in tumor progression and survival and has become the objective of intensive HTS and fragment-based screening campaigns.[25,26] The study of Bcl-x_L by noncovalent MS has not previously been reported, and this work therefore represents the first analysis of this potential therapeutic target by nano-ESI MS. The mass spectrometry results reported here have been validated using orthogonal data derived from ITC, ligand-observe (saturation transfer difference (STD) and two-dimensional nuclear Overhauser enhancement spectroscopy (NOESY)), and protein-observe ($^1H/^{15}N$ HSQC) NMR experiments. We propose that mass spectrometry can be a valuable additional tool for detecting noncovalent protein ligand interactions and has the sensitivity and dynamic range necessary for its application as a primary screen in FBDD.

RESULTS

Optimizing Sample Preparation and Spectrometer Parameters. Critical to the successful detection of weakly bound species is attaining spectra with adequate signal-to-noise (S/N) values. Good sample preparation is key to achieving this and is determined by the choice of buffer, desalting procedure, and protein concentration. Most buffers used for protein purification and storage are not compatible with ESI MS as they contain nonvolatile salts that are detrimental to the desolvation process required to transfer intact molecules into the gas phase. Purified proteins form weak electrostatic complexes with alkali metal cations resulting in ion suppression, peak broadening, and a corresponding reduction in mass accuracy. A buffer exchange step is therefore required prior to data acquisition.[27] There are several commercial systems available that can perform this task including dialysis, gel filtration, and membrane ultrafiltration. Factors including initial protein concentration, speed of buffer exchange, dilution effect, and sample loss will dictate the technique used.[27] In the work described in this study, large volumes were desalted by dialysis into the volatile buffer, ammonium acetate, whereas small volumes were successfully desalted in a single cycle into the same buffer using Micro Bio-Spin (Bio-Rad) or Zeba spin (Thermo Scientific) desalting columns (7K MWCO).

Aqueous ammonium acetate is the most common choice of buffer as sodium and potassium adducts are very readily exchanged with ammonium ions, resulting in simpler, more easily interpretable mass spectra. The concentration of ammonium acetate used, however, needed to be carefully chosen depending on the target protein. Effects of buffer concentration on the mass spectra of both hen egg white lysozyme and Bcl-x_L are shown in Figure 1A,B. Lysozyme is a small, globular protein that has been routinely analyzed under nondenaturing conditions (10 mM ammonium acetate), giving spectra with the +8 charge state as the most intense signal.[28] Figure 1A indicates that high-quality spectra for lysozyme could be obtained in the presence of between 10 and 75 mM ammonium acetate, replicating the dominant charge states seen in previous studies. Above 1 M ammonium acetate the proportion of adducts increased, reducing the S/N ratio, whereas at 3 M the +7 charge state became the most intense. Although this may be indicative of a more stable conformation, peak broadening renders these analytical conditions useless for mass analysis. Unlike lysozyme, there is no literature precedent for the analysis of Bcl-x_L by ESI MS. We utilized a biologically active deletion mutant of Bcl-x_L lacking the flexible loop region (Met45−Ala84) that has also been shown to be amenable to NMR studies.[29] The appearance and quality of ESI mass spectra obtained were highly sensitive to changes in buffer concentration (Figure 1B). A spectrum with good S/N and resolution was obtained at a buffer concentration of 25 mM, and at concentrations up to 100 mM spectra remained well resolved with only a small loss in S/N. Reducing the concentration to 5 or 10 mM, however, had a detrimental impact on sample desolvation, and peaks appeared broader. At low buffer concentrations the +8 charge state was the most intense, whereas at the higher buffer concentrations tested the intensity of the +9 charge state increased, suggesting an unfolding of the overall Bcl-x_L structure. At 20 mM ammonium acetate (pH 6.8) both lysozyme and Bcl-x_L gave well-resolved spectra with good S/N values, and these conditions were used in all subsequent experiments. The observed mass for lysozyme under these conditions was 14303 Da (expected mass 14302 Da), whereas the truncated Bcl-x_L gave a mass of 21296 Da (expected mass 21294 Da). The effect of protein concentration on signal intensity was also studied, with adequate S/N ratio and low sample consumption being the primary requirements (Figure 1C,D). Although lysozyme had a higher response than Bcl-x_L, a concentration of 10 μM was chosen for both proteins as a good compromise between sample conservation and reasonable S/N ratio.

The ability to perform nano-ESI MS is a prerequisite for routine analysis of macromolecular complexes.[30] The use of individual pulled borosilicate capillaries does not, however, allow for high sample throughput, and problems with poor reproducibility of signal intensities have been reported.[21] In this study a TriVersa NanoMate (Advion) robotic nanospray source was used. Sample was aspirated with a single-use pipet tip and sprayed through an individual nozzle on a NanoMate chip, containing a 20 × 20 array of 5 μm internal diameter nozzles. The single-use nature of the system (nozzles and tips) ensures that there is no sample carry-over between analyses, spray stability is good (average %RSD on 10 test samples of 2%), and signal intensity is equivalent to that achieved using pulled capillaries.[31]

To detect noncovalent protein−ligand complexes and determine accurate K_D values by mass spectrometry, instrumental parameters must also be carefully adjusted to minimize the effects of in-source dissociation and optimize ion transmission.[32] Failure to adequately adjust conditions precludes detection of weakly bound complexes and gives K_D values that are artificially high. This is of particular relevance to the detection of fragment binding as these interactions are characteristically weak, with K_D values that typically lie in the low micromolar to 1 mM range.[1] Spectrometer conditions (voltages, temperatures, and pressures) were iteratively optimized to soften the electrospray process and allow transmission of intact noncovalent complexes through the mass spectrometer. Of particular importance for the detection of fragment binding was the pressure in the source and analyzer region of the instrument. The effects of elevated pressure in the initial vacuum stages of the mass spectrometer, which provides collisional cooling for macromolecules, has been noted previously by other groups[33,34] and was adjusted here using a Speedivalve (Edwards Ltd., Sussex, U.K.) connected between the rotary pump and source pumping line. The pressure was increased to 4.65 and 2.5 × 10^{-6} mbar in the source and analyzer regions, respectively, appreciably reducing levels of in-

dx.doi.org/10.1021/jm201347k | J. Med. Chem. 2012, 55, 837−851

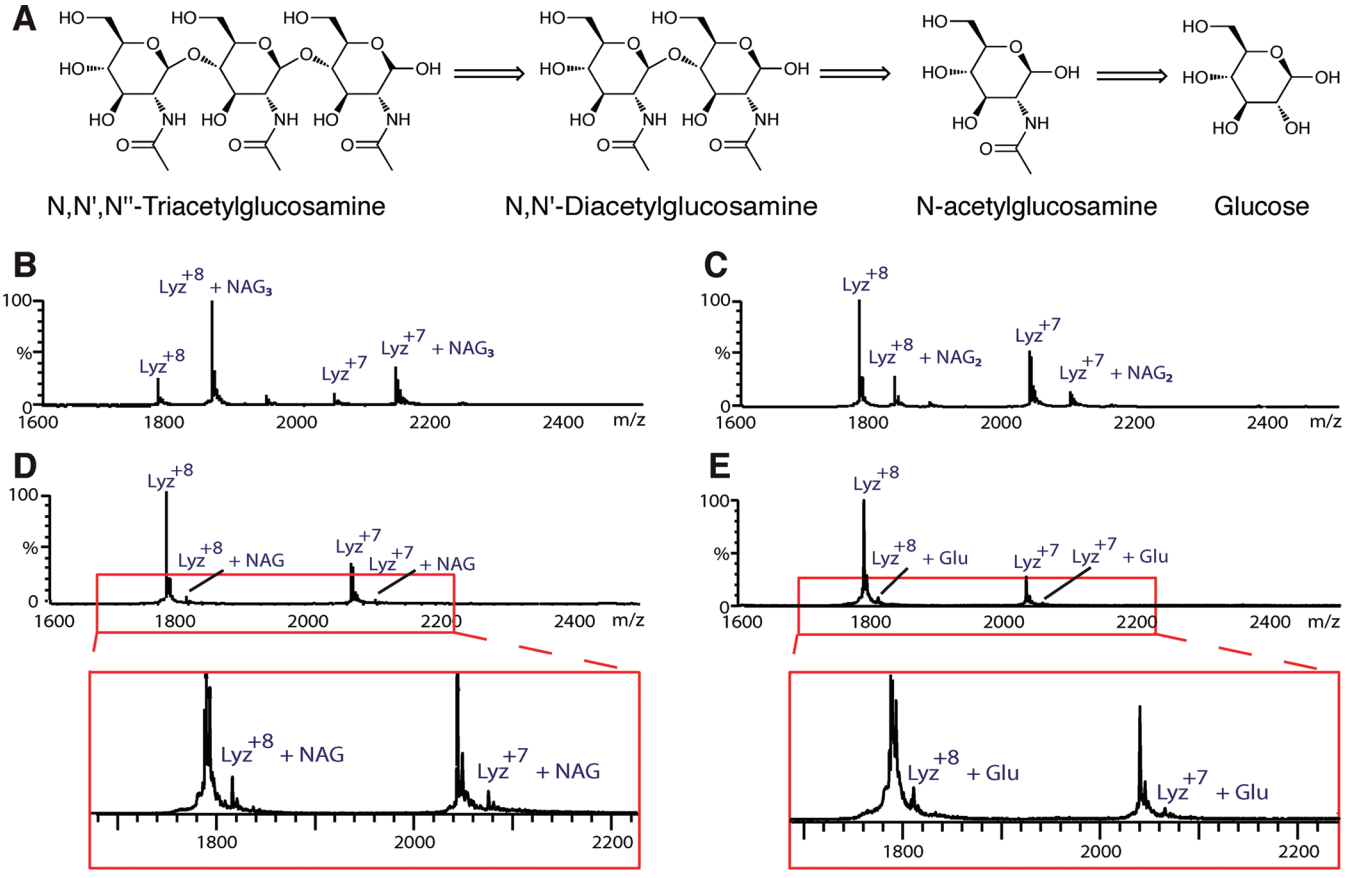

F

	K_D by nano ESI-MS	K_D by ITC	STD-NMR
Lysozyme + NAG_3	14 ± 2 μM	11 ± 0.4 μM	Positive
Lysozyme + NAG_2	229 ± 35 μM	189 ± 11 μM	Positive
Lysozyme + NAG	1000 ± 300 μM	N.D.[a]	Positive
Lysozyme + Glucose	5000 ± 400 μM	N.D.[a]	Negative

Figure 2. (A) Deconstruction of a strong binder to lysozyme, NAG_3, into its constituent fragments. (B–E) Mass spectra of lysozyme in complex with NAG_3, NAG_2, NAG, and glucose, respectively, focused on the +8 and +7 charge states. The concentration of lysozyme is 10 μM for all spectra shown, whereas the ligand concentration is 50 μM for spectra B–D and 150 μM for spectrum E. The panels below spectra D and E are enlargements of the area shown for clarity. (F) Binding results for each compound measured by MS, ITC, and STD-NMR.

source dissociation and allowing the identification of millimolar fragment binding. The source pressure used here is similar to that used in a previous study.[35]

To perform a blind screen of a fragment library, it was necessary to use a separate, well-characterized test system to ensure that under the conditions used, a series of compounds covering a range of K_D values (including weak binders) could be detected and that the K_D values measured by MS agreed with those obtained by orthogonal biophysical techniques. A rapid test carried out prior to screening a full library also indicates the limits of detection and the extent of in-source dissociation. Lysozyme was chosen as the protein standard, and *N,N′,N″*-triacetylglucosamine (NAG_3), a known, strong binder for this protein, was deconstructed into its constituent parts to provide four compounds that decrease in both size and binding affinity. Successive removal of two saccharide units from NAG_3 produces NAG_2 and NAG, respectively, whereas removal of the acetamido group leaves glucose (Figure 2A). Each of these compounds was incubated with lysozyme at ligand/protein (L/P) concentration ratios of 5:1 with the exception of glucose, which required a higher ratio of 15:1 to detect binding (Figure 2B–E). In agreement with previous studies, NAG_3 showed strong signals for both the +8 and +7 charge states for the noncovalent lysozyme–polysaccharide complex (Figure 2B).[28] NAG_2, a major hydrolysis product of the enzyme's natural substrate, NAG_6, and a competitive inhibitor of lysozyme, is known to bind much less strongly, and this was reflected in the levels of noncovalent complex observed (Figure 2C). Expanded regions are shown for two of the fragments analyzed, NAG and glucose (Figure 2D,E), to demonstrate that the S/N ratio was high enough to allow for accurate measurement of low levels of the complex. The slightly lower S/N ratio observed in Figure

dx.doi.org/10.1021/jm201347k | J. Med. Chem. 2012, 55, 837–851

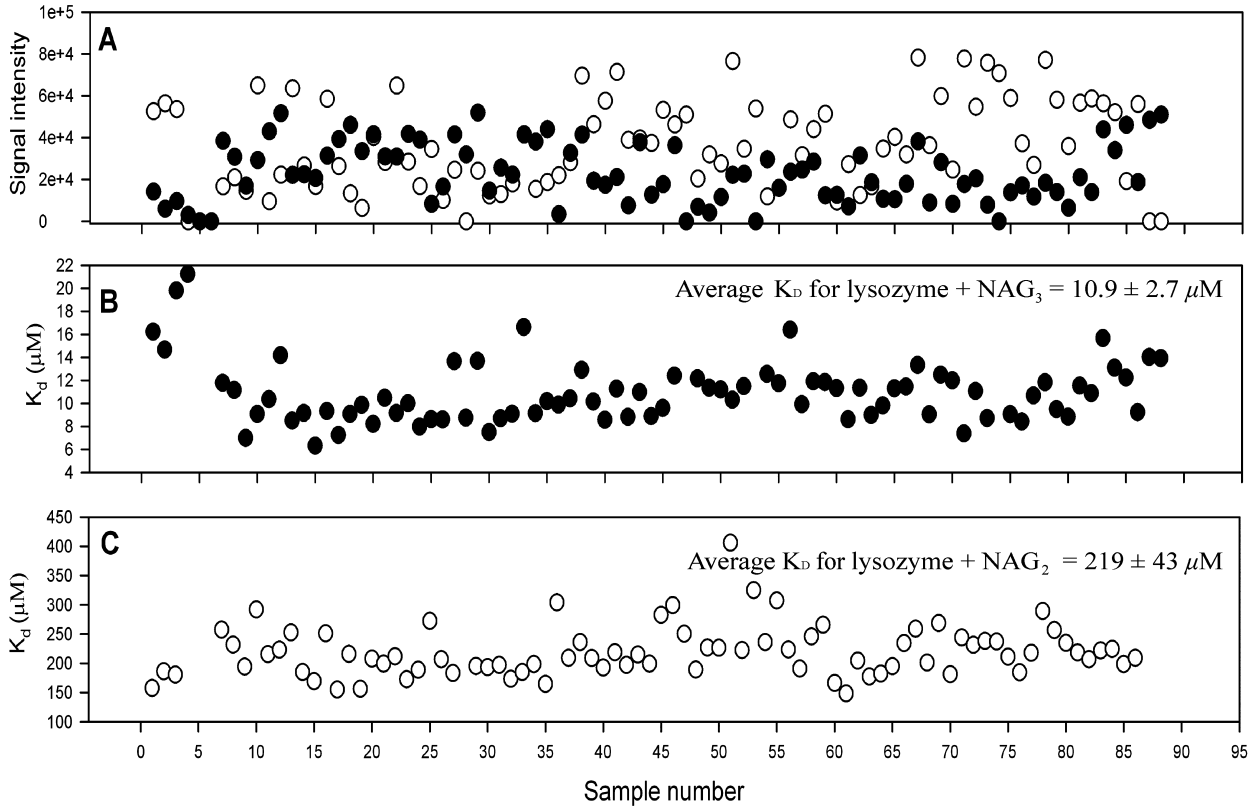

Figure 3. (A) Variation in signal intensity from an MS screen of repeating, identical samples of lysozyme (10 μM) plus NAG_3 (50 μM) (solid circles) or NAG_2 (100 μM) (open circles). (B) Variation in K_D across lysozyme−NAG_3 samples. (C) Variation in K_D across lysozyme−NAG_2 samples.

2E is due to the 3-fold increase in ligand concentration used to record this spectrum. Cross-validation of the lysozyme−NAG_n binding was achieved using two orthogonal techniques, ITC and STD-NMR (Figure 2F and Figures S1 and S2 in the Supporting Information). The K_D for NAG_3 binding was measured by MS titration at 14 μM and compares well with that obtained by ITC in this study (11 μM) as well as published values measured by MS, fluorescence, and ultraviolet (UV) spectroscopy.[36−38] The measured K_D of 229 μM by MS for the lysozyme−NAG_2 complex is also in excellent agreement with that obtained by ITC (189 μM) and is consistent with published work. Additionally, MS was able to detect binding of the fragment-sized compound, NAG, to lysozyme with a measured K_D of 1 mM. ITC was unable to detect millimolar affinity binding in this case, although binding was detected by STD-NMR, indicating that the MS analysis had correctly identified binding of this compound. Binding of glucose to lysozyme was not detected by either STD-NMR or ITC, although MS analysis identified an interaction with a K_D of 5 ± 0.4 mM.

Development of an Automated Nano-ESI MS Screen. Full automation of the MS method is necessary to achieve high throughput and full, unattended compound library screening. A 384-well plate was prepared with alternating rows of protein and ligand solutions using a fluid-handling robot. The NanoMate was then programmed to aspirate 10 μL of ligand solution, dispense this into a protein-containing well, mix the solution, and then aspirate 5 μL, which was then sprayed into the mass spectrometer for 30 s. The spectrometer was linked to the NanoMate via a contact closure to trigger data acquisition for each sample. Subsequent automated deconvolution of the raw data was performed using the MaxEnt algorithm within BiopharmaLynx software (Waters).

To evaluate the reproducibility of the screening method, both strong (NAG_3) and weak (NAG_2) binders to lysozyme were used. Alternate rows of a 384-well plate were filled with lysozyme, whereas the remaining wells were filled with alternating NAG_3 and NAG_2 samples. This gave a total of 94 individual experiments for both NAG_3 and NAG_2. The fully automated analysis took 6 h to screen all samples (100 s per sample), including approximately 1 h for postacquisition data processing. For each sample both the signal intensity and the measured K_D value were recorded. Figure 3A shows the resulting plot of sample number versus signal intensity for both NAG_3 (solid circles) and NAG_2 (open circles), whereas panels B and C of Figure 3 plot sample number versus K_D value. The signal intensity was measured as the sum of the peak intensities for free protein plus the protein−ligand complex and shows variation across the screen. No trend was observable, however, to suggest that screen performance deteriorated over time. It is apparent from the signal intensities given in Figure 3A that a proportion of samples (~5%) failed to spray due to blockage of the NanoMate chip nozzles. This proportion was reduced from a higher initial failure rate by sealing the plate with a pierceable foil cover to prevent evaporation and subsequent concentration of analyte. In addition, plate centrifugation prior to screening was used to sediment particulates that could also cause nozzle blockage. Previous studies have noted a similar low blockage rate for the automated chip-based system,[21] although this remains significantly less problematic than blocking of pulled capillaries. Despite the variation in signal intensity, the K_D values measured in Figure 3B,C remained uniform across the

dx.doi.org/10.1021/jm201347k | J. Med. Chem. 2012, 55, 837−851

screen and were in excellent agreement with the K_D values recorded during the initial MS analysis of the NAG_n system (Figure 2F).

Nano-ESI MS Screening of a Targeted Library of Phenylpyrazole-Derived Compounds against Bcl-x_L. Compounds based around a phenylpyrazole moiety have previously been identified as having activity against the anti-apoptotic Bcl-2 protein family (of which Bcl-x_L is a member).[39] This was therefore selected as a central scaffold for the assembly of a targeted library against Bcl-x_L. This compound library was expected to include a significant number of binders and therefore acted as a convenient validation of the MS screening protocol. The scaffold used (**1**) has two points of diversity (R_1 and R_2, Figure 4) to which a variety of functionalities were attached, generating a final library containing 157 compounds. The compounds varied in MW from 240 to 500 Da and so, by conventional nomenclature, range from large fragments to full-sized molecules.[40,41] An experimental $LogD_{7.4}$ measurement was made for all compounds and varied from −0.72 to 3.83.

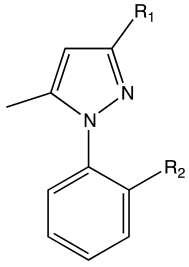

Figure 4. Structure of the phenylpyrazole scaffold (**1**) around which a library of 157 compounds was assembled. R_1 and R_2 are points of diversity to which different chemical functionalities were attached.

K_D measurements made from a single point will be accurate only for ligands with K_D values close to the concentration of the ligand used. Protein binding sites begin to saturate at low values of $[L_0]$ for strong binders, whereas weak binders require high $[L_0]$ values to accurately determine a K_D value. The choice of ligand concentration used for a single screen by MS will, therefore, constrain the range of K_D values that can be accurately measured. This can be illustrated using simulated binding curves assuming a single binding site and ligand species (Figure S3, Supporting Information). These simulations demonstrate that at a protein concentration of 10 μM and a L/P ratio of 2:1, a significant proportion of protein is in a complex with the ligand for K_D values in the range of 10−200 μM. At this L/P ratio experimental error in determining the fraction bound, [PL], leads to relatively small changes in the determined K_D. For K_D values >200 μM, the binding response is weak, and only a small proportion of [PL] would be formed. In this region of the graph even small errors in the measurement of [PL] lead to large changes in the estimated K_D. For stronger binders with K_D values <10 μM, the MS assay detects binding but saturation of the protein binding sites gives an underestimation of the K_D. This was tested experimentally using lysozyme and NAG_2. NAG_2 was titrated from 10 to 1600 μM at a constant protein concentration (10 μM, Figure 5), and the K_D value calculated by curve-fitting the data was 197 ± 60 μM. For single-point calculations at low ligand concentrations, the K_D was estimated at 142 μM (L/P 2:1) and at 621 μM (L/P 160:1). Therefore, as expected, a K_D of the order of 200 μM could be reasonably estimated by a single 2:1 (L/P) ratio measurement.

A L/P ratio of 2:1 was therefore chosen to explore the range of protein−ligand interactions that could be detected while minimizing the consumption of ligand and limiting the occurrence of false positives. The results of this screen are given in Figure 6. Several combinations of R_1 and R_2 groups were not synthetically viable for this library and have been left blank. Approximate K_D values were calculated from the ratio of free protein to protein−ligand complex. This allowed compounds to be grouped according to their apparent affinity

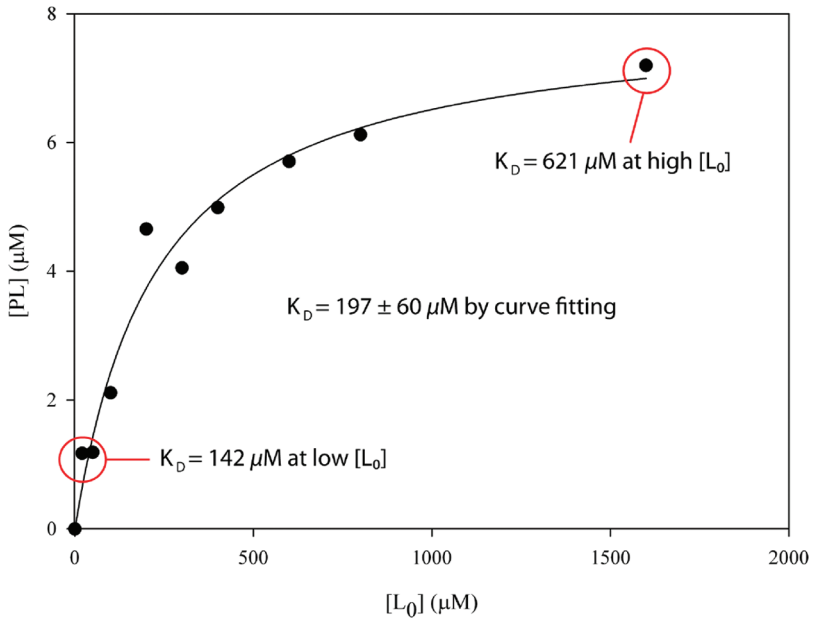

Figure 5. Variation in protein−ligand (PL) complex formed as initial ligand concentration $[L_0]$ is increased. Data shown were obtained with lysozyme (10 μM) and NAG_2. The amount of complex observed begins to plateau, above which increased ligand concentration no longer increases complex formed.

dx.doi.org/10.1021/jm201347k | J. Med. Chem. 2012, 55, 837−851

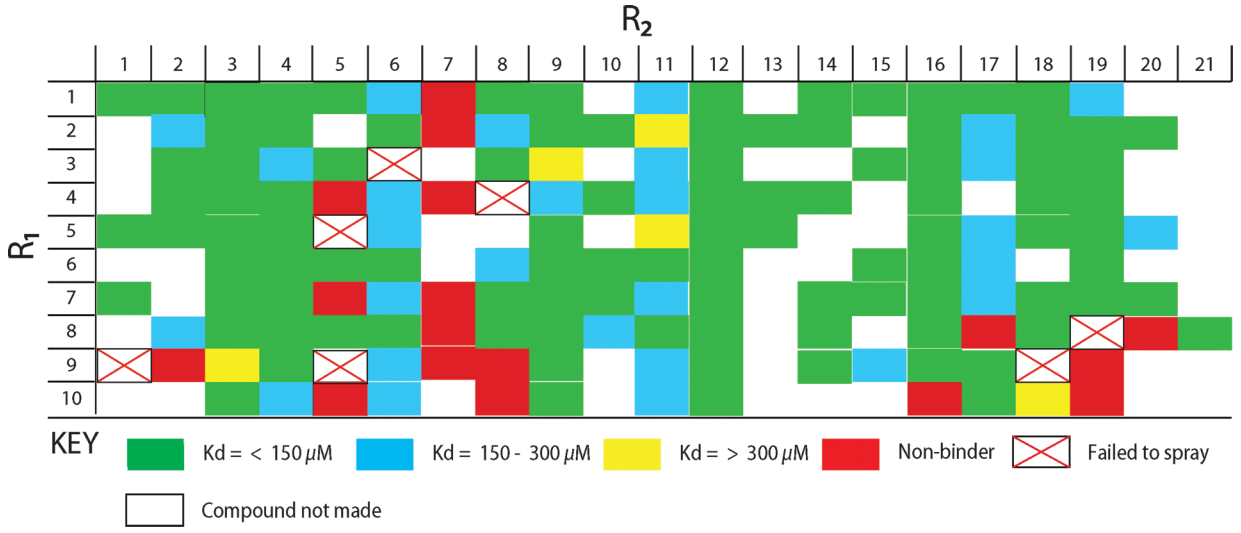

Figure 6. Results from the MS screen of a library of phenylpyrazole-derived compounds against Bcl-x_L at a 2:1 ligand/protein ratio. Each row corresponds to a different chemical functionality at R_1 and each column to a different chemical functionality at R_2. Compounds have been color-coded according to their measured K_D values and are grouped as shown in the key.

for Bcl-x_L (K_D < 150 μM (green), K_D = 150−300 μM (blue), and K_D > 300 μM (yellow)).

Controls were inserted into every 10th position on the 384-well plate to report screen performance. The controls alternated between lysozyme/NAG_3 and Bcl-x_L plus a known binder, **2** (UCB1319870). Lysozyme/NAG_3 provided an independent control, whereas Bcl-x_L/**2** allowed verification that the target protein remained biologically active over the time taken to screen. On each plate, the average K_D value was calculated from the resulting eight data points collected for each pair of controls (Table 1). Single-point measurements of K_D values obtained for both lysozyme/NAG_3 and Bcl-x_L/**2** indicated that consistent results were observed during a single screen as well as between screens recorded on separate days. The standard deviation between control K_D values was low (16 ± 4 and 141 ± 23 μM for lysozyme/NAG_3 and Bcl-x_L/**2**, respectively). For the lysozyme/NAG_3 K_D this single-point estimation compares well with the value obtained from a five-point titration curve (Figure 2F).

Table 1. Summary of Results from the Controls Added to All MS Screens[a]

screen	K_D of Bcl-x_L + **2** (μM)	K_D of lysozyme + NAG_3 (μM)
1	163 ± 85	21 ± 6
2	118 ± 33	14 ± 5
3	143 ± 53	13 ± 5

[a]The K_D values are taken as an average of the eight data points collected for each control during the screen. The error given is the standard deviation between the eight data points.

The MS screen detected binding across a range of apparent K_D values (approximately 30−400 μM) for the phenylpyrazole library and also distinguished nonbinding compounds. The limit of detection was determined as the lowest [PL]/[P] ratio that could be reliably measured during the screen. This was 0.07 for the 10 mM protein concentration used in the MS screen described. Of the 157 compounds tested, 66% were identified with K_D values <150 μM and 18% between 150 and 300 μM, with 2% above 300 μM; 9% were nonbinders, and 4% failed to spray. Each ligand-binding category incorporated a wide range of both mass and hydrophobicity. From the 14 (9%) nonbinding compounds, 6 were poorly soluble. For the remaining nonbinders there was no correlation with hydrophobicity, with $LogD_{7.4}$ values ranging from 0.67 to 2.6 (Supporting Information, Figure S4). This initial screen was repeated to evaluate the reproducibility of results. There was a 97% agreement in compounds identified as hits, and 63% of compounds exhibited <30% error in K_D values between screens. To assess the MS assay at higher ligand concentrations, L/P ratios at 4:1 and 8:1 were also screened (Figure S5, Supporting Information). At a L/P ratio of 4:1 the number of compounds with K_D values <150 μM now fell to 15%, whereas 33% were between 150 and 300 μM and 16% were >300 μM. Further increasing the L/P ratio to 8:1 now indicated that 3% of the compounds tested had K_D values below 150 μM, with 41% between 150 and 300 μM and 17% > 300 μM. The failure to spray rate, however, increased in both of these experiments (19% at 4:1 and 33% at 8:1) and was attributable to the increased likelihood of more concentrated ligand forming blockages when sprayed through the NanoMate nozzles. The full screen of 157 compounds consumed only 668 μg of protein and 44 μg of ligand (at a 2:1 L/P ratio) and took 100 s per sample to complete data acquisition.

Validation of MS Screen Results Using ITC, STD-NMR, and Chemical Shift Perturbations. To validate the hit rate observed in the 2:1 L/P MS screen, a subset of 20 ligands was selected from the targeted phenylpyrazole-derived library and assessed using four complementary, orthogonal techniques. These compounds covered a range of MS K_D values, including nonbinders (Table 2). 2D-NOESY, STD-NMR, and ITC were used to verify the MS screening results, whereas chemical shift perturbations (CSP) measured by $^1H/^{15}N$ heteronuclear single-quantum coherence (HSQC) NMR titrations were used to locate the binding site. STD-NMR is a well-established technique for protein−ligand screening and hit identification,[42] whereas ITC remains the "gold standard" for K_D and thermodynamic measurements.[43] Comparison of chemical shift changes measured by $^1H/^{15}N$ HSQC NMR experiments in the absence and presence of ligand can identify the site of ligand binding on the protein surface and confirm the

dx.doi.org/10.1021/jm201347k | J. Med. Chem. 2012, 55, 837−851

Table 2. Comparison of MS Results with Orthogonal Techniques, 2D-NOESY, STD-NMR, and ITC, for a Subset of 20 Compounds (1a−t) from the Phenylpyrazole Library against Bcl-x_L[a]

Compound ID	MW	LogD (7.4)	2D-nOesy Aggregation	MS K_D (μM)	STD-NMR enhancement	2D-NOESY binding	ITC K_D (μM)
1440115 (**1a**)	401.4	0.53	No	57/181 (185, 103)	Yes	Yes	77 ± 47
1440022 (**1b**)	258.3	1.42	No	71/187 (261, 263)	Yes	Yes	4 ± 4**
1440078 (**1c**)	404.5	0.46	No	114/139 (fail, 368)	Yes	*	8 ± 12**
1440048 (**1d**)	308.4	0.24	No	101/fail (88, 286)	Yes	*	2 ± 1**
1440138 (**1e**)	321.3	0.68	No	102/107 (fail, 203)	Yes	Yes	52 ± 35
1440154 (**1f**)	370.4	1.45	No	75/166 (105, 165)	Yes	Yes	13 ± 5
1440003 (**1g**)	322.4	0.2	No	87/92 (fail, 154)	Yes	No	43 ± 19
1440043 (**1h**)	414.5	1.53	No	100/81 (fail, 135)	Yes	Yes	17 ± 12
1440124 (**1i**)	379.4	0.87	No	103/200 (110, 149)	Yes	Yes	54 ± 63**
1440110 (**1j**)	312.4	1.23	No	80/81 (107, 208)	Yes	No	60 ± 40
1440077 (**1k**)	484.5	0.55	No	42/70 (125, 227)	Yes	Yes	31 ± 39**
1440047 (**1l**)	365.4	0.78	No	302/142 (217, 645)	Yes	Yes	412 ± 75
1440075 (**1m**)	335.4	1.32	No	181/205 (245, fail)	Yes	Yes	NB
1440094 (**1n**)	312.4	1.31	No	306/148 (249, fail)	No	*	NB
1440072 (**1o**)	340.4	1.55	No	192/264 (393, 1123)	Yes	No	NB
1440829 (**1p**)	341.4	-	Yes	397/212 (341, fail)	No	No	ND
1440063 (**1q**)	517.6	2.46	Yes	237/NB (NB, NB)	No	No	ND
1440046 (**1r**)	478.5	1.28	Yes	36/49 (NB, NB)	No	No	ND
1440037 (**1s**)	312.4	3.45	No	295/NB (NB, NB)	No	*	ND
1440019 (**1t**)	334.4	2.76	Yes	NB/229 (NB, NB)	No	No	ND

[a]Data on compound MW and $LogD_{7.4}$ are also given, and compounds that showed poor solubility in an AKAS solubility assay are shaded. MS K_D values are given for both screens performed at a 2:1 ligand/protein ratio. Numbers given in parentheses are K_D values calculated from screens at ratios of 4:1 and 8:1, respectively. NB denotes a nonbinder. ND denotes not determined. * denotes a signal change that was too small to unambiguously identify binding to the protein. ** denotes a K_D that was poorly determined due to low heats of binding at the sensitivity limit of the ITC instrument.

specificity of binding.[42] Standard 2D-NOESY was used to identify ligand aggregation.[44] Small molecules are expected to give positive NOEs, whereas negative NOEs, resulting from slow molecular tumbling, may signify the formation of higher order aggregates. Aggregating compounds are likely to give anomalous results in binding assays (Supporting Information, Figure S6). Four compounds were identified as aggregating in solution. One of these, **1t**, had already been identified as poorly soluble in a separate solubility assay and showed no binding by MS. Two further compounds, **1q** and **1r**, showed poorly reproducible binding by MS, but were not highlighted as insoluble in the assay. The remaining aggregating compound, **1p**, was the weakest binder identified by MS.

STD-NMR was employed as a ligand-detect NMR experiment where enhancement of the ligand signals in the presence of the target protein provides a qualitative indication of binding.[5] A comparison between the MS and STD-NMR data (Table 2) revealed that 19 of the 20 compounds tested by STD-NMR were in good agreement with the MS data (disregarding **1p** due to aggregation). Compound **1n** failed to give an STD-NMR response, although MS analysis indicated a weak interaction. Compounds that bind upon addition of protein can also be characterized by a change in NOE sign from positive to negative in the 2D-NOESY experiment as the small molecule adopts an NOE buildup characteristic of the protein.[42] Broadly, the 2D-NOESY assay was in agreement with both MS and STD-NMR results, although the number of false negatives was higher as NOE buildup for weakly interacting ligands may not be sufficient to significantly perturb the sign of the NOE.

A single STD-NMR experiment does not provide a quantitative estimation of the protein−ligand interaction. This technique is also insensitive to very strong (nM K_D) interactions. ITC was, therefore, used to determine quantitative information regarding the dissociation constants and thermodynamic parameters for each interaction.[43] Initial ITC experiments were conducted using sample concentrations of 100 μM protein and 1 mM ligand. The relatively weak interactions and very low enthalpies of binding for these compounds, however, made K_D determination difficult (Supporting Information, Figure S7). To overcome this, the concentration of reagents used was increased to 150 μM protein and 2 mM ligand. These were the maximum concentrations that maintained ligand solubility and achieved saturation of protein binding sites. When data were obtained by ITC (15 of the 20 compounds tested), 7 gave K_D values similar to those determined by MS analysis. For the remaining 5 compounds, low injection heats complicated data analysis. Despite a clearly sigmoidal binding curve, the error on the calculated K_D value after curve fitting was so large as to preclude an absolute determination of the binding constant. A further 3 compounds showed no binding isotherm by ITC and very weak binding by MS. ITC experiments were not conducted for the final 5 compounds in Table 2 due to low solubility at the elevated concentrations required for the assay.

The location of compound binding was evaluated using $^{1}H/^{15}N$ HSQC experiments and compared with the published structure of Bcl-x_L in complex with the natural Bak peptide ligand.[29] Complete backbone chemical shift assignments were obtained using a $^{13}C,^{15}N$-labeled sample of Bcl-x_L in

dx.doi.org/10.1021/jm201347k | J. Med. Chem. 2012, 55, 837−851

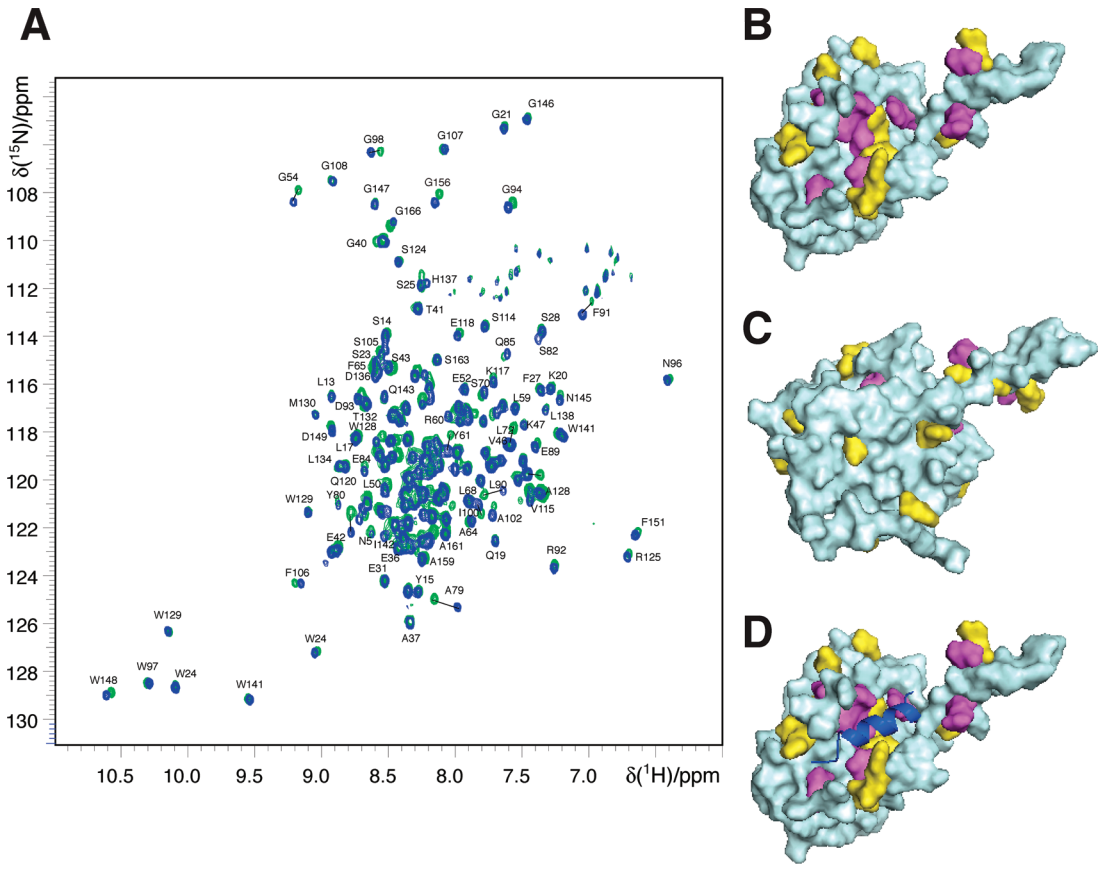

Figure 7. (A) $^{1}H/^{15}N$ HSQC of uniformly ^{15}N-labeled Bcl-x_L with only partial assignments shown for clarity. Peak migration after addition of compound **1a** is shown by superposition of HSQC spectra from the free form (blue) to the bound form (green). (B) Weighted chemical shift variations $\Delta\delta_{av}$ due to binding of **1a** are indicated on the surface of the Bcl-x_L structure according to the following code: $\Delta\delta_{av} \geq 0.1$ ppm, magenta; $0.1 \geq \Delta\delta_{av} \geq 0.05$ ppm, yellow. (C) The structure of Bcl-x_L in panel A was rotated by 180°, illustrating that shifts are localized around a single binding pocket. (D) Bcl-x_L in complex with a natural peptidic inhibitor (Bak) shown in blue illustrates the location of the binding cleft on Bcl-x_L.

combination with a suite of standard triple-resonance assignment NMR techniques. ^{15}N-labeled Bcl-x_L spectra were then obtained in the presence and absence of an excess of ligand. Four compounds from Table 2 were selected to span a range of affinities for Bcl-x_L from the MS screen (**1a**, **1f**, **1b**, and **1j**). All four compounds displayed similar chemical shift perturbation patterns. Figure 7A shows superimposed $^{1}H/^{15}N$ HSQC spectra of Bcl-x_L with and without the addition of **1a**. Several distinct CSPs were observed between the free (blue) and bound (green) forms of Bcl-x_L and **1a**. The weighted average chemical shift differences ($\Delta\delta_{av}$) were calculated for each residue on compound binding and were mapped onto the solution structure solved previously for Bcl-x_L (Figure 7B).[29] Residues were colored according to the following code: $\Delta\delta_{av} \geq 0.1$ ppm, magenta; and $0.1 \geq \Delta\delta_{av} \geq 0.05$ ppm, yellow. There was a distinct group of CPSs localized around one region corresponding to the known interaction site (Figure 7B). Rotating the structure by 180° (Figure 7C) reveals that several CSPs were observed distal to this site, but they are not clustered and may be due to secondary effects upon ligand binding. The binding mode of a natural peptidic inhibitor, Bak (PDB accession code 1BXL),[29] is shown in Figure 7D. The CSPs produced by binding of **1a** were clustered and overlapped with the known binding site of Bak. This demonstrated that the interaction of the ligand is specific and located in the desired binding cleft.

DISCUSSION AND CONCLUSIONS

Screening is an expensive process, and it is estimated that up to U.S. $1 000 000 may be spent analyzing a library of 1 000 000 compounds.[45] A range of experimental approaches is required, with X-ray crystallography being the highest resolution, most information-rich technique. Similarly, NMR can provide interaction data and localize ligand-binding sites. Both of these methods require significant capital investment, incur high running costs, and need dedicated expertise for data analysis. Complementary techniques are therefore required to provide preliminary binding data, which can filter potential leads into X-ray and NMR studies for SAR. Typically, ITC and SPR fulfill this role, although both have drawbacks. ITC may be less useful as a front-line screen due to poor signal response with weakly binding ligands, high sample consumption, and low throughput.[43] SPR requires immobilization of one of the interacting partners, which may not achievable. Even if immobilization is possible, this could potentially affect the binding interaction and lead to additional nonspecific association and surface effects. Ligand detect NMR binding assays have emerged as rapid, low protein consumption techniques, which have been used as first-pass screens. Mass spectrometry can act as an orthogonal method as it is both fast and sensitive and provides a direct measure of binding stoichiometry. Noncovalent mass spectrometry has been developed over the past 20 years, and many of the technical issues required for its routine application have been resolved. To date, a number of screens with small

dx.doi.org/10.1021/jm201347k | J. Med. Chem. 2012, 55, 837−851

compound libraries have been reported with a detection limit of approximately 100 μM.[32] This methodology is acceptable for compounds in which a significant binding affinity has already been achieved, however, the current trend is toward fragment library screening, where binding may be an order of magnitude weaker. To detect these millimolar strength complexes, the use of high ligand/protein ratios and extensive adjustment to the experimental protocol are required.[46,47] The aim of this study was therefore to investigate the applicability of MS for performing high-throughput screening. A screen by nano-ESI MS was developed using an Advion TriVersa NanoMate and an LCT Premier mass spectrometer (Waters) to fully automate analysis of a compound library and generate an experimental protocol under which a range of binding affinities could be routinely detected by MS. The screening of a large sample library requires unassisted and reliable sample handling and delivery followed by automated data acquisition. The NanoMate robotic nanospray source can be interfaced with a number of different mass spectrometers to achieve this. Spectrometer conditions (voltages, temperatures, and pressures) were iteratively optimized to soften the electrospray process. Increasing the spectrometer pressure was of paramount importance for the detection of weakly bound ligands. This was done using a Speedivalve for manual pressure adjustment. Collisional cooling may be achieved by the introduction of an ion guide on other instruments.

We selected lysozyme as a model protein as it is a small robust enzyme that has been extensively studied using noncovalent mass spectrometry conditions.[28] Lysozyme binding to NAG_n has also been well characterized using a range of biophysical techniques. Significantly, it is known to survive the electrospray process without loss of activity.[48] This enzyme−substrate complex is therefore a useful standard for comparison across different mass spectrometry platforms. As with other studies we found ammonium acetate to be a suitable volatile buffer. In the case of lysozyme, deterioration of signal intensity did not occur until molar concentrations of buffer were utilized. The anti-apoptotic protein Bcl-x_L has also been studied in biophysical screens[25,26] as a potential anticancer target.[49,50] To our knowledge, this is the first application of native mass spectrometry to this therapeutic target.

The use of the deconstructed NAG_n system allowed us to measure K_D values across a range of molecular weights and interaction strengths, achieving good agreement between MS, ITC, and STD-NMR. These values are consistent with previous results from automated ESI-chip and manual syringe infusion MS as well as UV and fluorescence measurements.[51] Although lysozyme shows optimum enzyme activity at pH 5,[52] MS determinations of NAG_3 and NAG_2 binding at pH values ranging from 5.2 to 8.2 show little difference in ligand binding strength.[36,51] The lysozyme control can therefore allow a pH to be chosen for screening that suits the target protein. The K_D for lysozyme/NAG was determined to be 1 mM, although, in previous work, this complex was reported to be too weak to detect using mass spectrometry.[28] Other compounds with millimolar affinities have been detected previously using this technique,[46,47] but this is not routine. ITC did not detect the millimolar lysozyme/NAG interaction, although we confirmed binding using STD-NMR. Binding has also been observed in other studies (UV, differential scanning calorimetry, and fluorescence) and a wide range of affinities reported (mM−M),[37,38,53−55] albeit with a weaker interaction than we have determined by MS. MS identified an interaction of glucose with lysozyme with a K_D of 5 ± 4 mM, but only when the ligand/protein ratio was increased 3-fold. Glucose is not thought to bind to lysozyme as it lacks the *N*-acetyl group considered to be crucial for the interaction.[56] Binding was not detected by either ITC or STD-NMR. Association by MS at these high ligand concentrations is likely to be attributed to nonspecific gas phase complex formation.

Across the 5 h control screen of 94 lysozyme/NAG_3 and 94 lysozyme/NAG_2 complexes the K_D values showed RSD values of 25 and 20%, respectively, giving confidence in this screening method. These figures are comparable to those of previous studies that used smaller sample sizes than this study (Supporting Information, Table 1).[21,35] Signal intensity differences were observed that could be attributed to minor nozzle variations in the NanoMate chip and suboptimal automated chip positioning. This does not appear to affect the reproducibility of the K_D determined across the screen. The results from controls (lysozyme/NAG_3 and Bcl-x_L/**2**) inserted after every 10 samples during screening against Bcl-x_L (Table 1) also demonstrated that across a single or multiple screens, the K_D measurements showed little variation and agree with the values determined during initial optimization. By comparison, Bovet et al. report changes in the bound/free ratio of up to a factor of 3, whereas we observe variations of half this value.[35] In another screen of 23 compounds, theK_D or [P]/[PL] ratios were not reported.[19] We have therefore attained a high level of reproducibility, which has been achieved across a total of 180 individual nozzles over a period of 5 h. The failure to spray rate at a 2:1 L/P ratio was 4%, indicating that only a small number of samples might need to be reassessed.

Compounds based on a phenylpyrazole scaffold (**1**) have been previously shown to bind to several key protein subpockets normally occupied by hydrophobic residues of the helical Bak, Bad, and Bim peptides.[39] Variation of R_1 and R_2 on this scaffold gave IC_{50} values from 5 to 20 μM against the complex of Bcl-x_L and Bak 16-mer peptide. In our MS screen against Bcl-x_L we expected, therefore, to generate a substantial number of binding ligands with the current library. From simulations of the accuracy of the determined K_D for binders in the low to mid micromolar range at a protein concentration of 10 μM, we chose a ligand/protein ratio of 2:1 for the initial identification of bound compounds. The full screen was acquired at a rate of 100 s per sample and yielded a hit rate of 90%. A significant amount of time was required to perform the necessary initial experiments described here in terms of instrument setup and sample preparation. Once complete, however, the additional time required to adapt the method for a different protein or library would be reduced, and overall throughput for the screen by MS is competitive with other techniques including STD-NMR. The MS screen is also comparable in terms of sample consumption; a screen of 157 compounds consumed <1 mg of protein and only 44 μg of ligand. The corresponding screen by STD-NMR would have consumed approximately 20 times more protein and 250 times more ligand while taking over 15 times longer. It is possible to conduct fragment screening by NMR with similar sample consumption and higher throughput to the MS screen described here if fluorine chemical shift anisotropy and exchange for screening (FAXS) NMR experiments are conducted.[57] Using mixtures of fragments, this technique can achieve a throughput of over 1000 compounds in 24 h, although these experiments require fluorine-containing frag-

ment libraries. Screening by ITC would have required, however, a further 10-fold increase in material.

There are several factors that have hindered the acceptance of mass spectrometry-based screening. These include concerns about changes to solution phase equilibria during ESI, relative ionization efficiencies of free and complexed protein, and experimental time for K_D measurement by titration. Several studies have shown, however, that the solution phase equilibria can be reflected during ESI MS, and ionization efficiencies of free and complexed protein can also be assumed to be similar.[58] Lastly, a detailed study by Mathur et al. determined K_D values by ESI titration and other complementary techniques. Here they showed that recording titration curves in triplicate would take several hours per compound.[59] This would make mass spectrometry an unsuitable technique for noncovalent screening procedures, and this approach has therefore been viewed as cumbersome and time-consuming. Our study shows that a single 2:1 ligand/protein ratio can, however, be used to rapidly identify a high proportion of binders and provide an estimation of binding strength. Extraction of approximate K_D values from the confirmed binders revealed that bound ligands were detected across a broad range (31−397 μM). It is expected that under these conditions, stronger binding in the low micromolar to millimolar range would be detectable, but as the simulation curves are almost identical in this range, the K_D values would not be well differentiated. Accurate determination of these K_D values would require very low protein concentrations that would not yield adequate sensitivity. Very weak binders were detected only at higher ligand concentrations. The dynamic range for any screen, therefore, is directly correlated with the initial ligand concentration used. Weaker binders could be either discarded in favor of any tighter binders identified or pursued in cases when no superior leads were found. For example, in the 2:1 L/P ratio screen, 17 compounds were identified as nonbinders. Four of these subsequently showed binding at a higher L/P ratio (8:1), indicating that these compounds were very weak binders.

The high hit rate observed in the 2:1 L/P screen may arise from detection of false positives due to nonspecific gas phase interactions forming during the electrospray process.[58,59] False positives or false negatives affect all screening methods to some extent, however, and additional screens using orthogonal techniques must be performed to confidently identify binding events. 2D-NOESY, STD-NMR, and ITC data were acquired on a subset of the compounds to confirm the MS binding data. ITC experiments that yielded binding curves were also used to derive K_D values, but this proved challenging even with a directed library due to weak ligand affinity and low binding enthalpies (see the Supporting Information, Figure S7). The error on several of the curve fits was therefore considered too high for a K_D value to be extracted. When the K_D values could be derived from ITC data, they were of the same magnitude as those determined by MS. Larger discrepancies occurred at the weaker end of the binding spectrum, where ITC might not be expected to detect binding without the use of competition-type experiments. Three compounds that displayed weak binding by MS were not identified as binders by ITC. However, the overall agreement between MS, STD-NMR, and ITC in terms of the identification of binders and nonbinders is compelling. For four compounds, CSPs from $^{1}H/^{15}N$ HSQC titration experiments were mapped onto the protein surface and confirmed that binding overlapped with the Bak peptide interaction site (PDB accession code 1BXL).[29] Determining the location of compound binding adds to the evidence that the hits identified from a high-throughput MS screen were correct and specific to a therapeutically relevant binding site. The structural similarity between the compounds screened allows the assumption to be made that this binding site is common to other compounds identified as hits by the MS screen.

Despite the similar scaffold, a number of physical properties show a large variation across the library. The $LogD_{7.4}$ values for each compound were measured to estimate the degree to which hydrophobic interactions might contribute to overall binding for each complex. A high $LogD_{7.4}$ value does not, of course, preclude additional stabilizing interactions such as hydrogen bonds, and a structure of each complex would be required to fully identify the important binding interactions. The compounds tested had $LogD_{7.4}$ values ranging from −0.72 to 3.83, and there was no observable correlation between the $LogD_{7.4}$ and the measured K_D, that is, no apparent bias against detecting more hydrophobic complexes (Supporting Information, Figure S4). The structural diversity is, however, limited by the common phenylpyrazole moiety, which may provide the predominant binding interaction and limit the potential role of R_1 and R_2. The weak binding enthalpies measured by ITC suggest that electrostatic interactions do not contribute greatly to the overall binding strength, and the binding interaction may therefore be predominately hydrophobic.[43] We also observed no correlation between the molecular weight and K_D, indicating that the MS screen identified binding interactions from compound sizes ranging from fragments to typical drug-sized compounds with no apparent bias.

Although a structure of each complex would be required to fully identify the interactions that are important for binding, the presentation of the MS screen data in Figure 6 already provides some preliminary SAR. There are identifiable trends where a particular group appears to confer either strong or weak affinities, regardless of the identity of the second substituent. For example, the addition of the R_2 group in column 7 precludes binding irrespective of the group at R_1. The compounds in this column range in $LogD_{7.4}$ from 0.24 to 2.6, suggesting that the lack of activity here is not associated with a gas phase weakening of hydrophobic interactions. Consistently low K_D values are found in columns 3 and 4, which is interesting because the R_2 groups for these two columns are highly related, whereas changes in R_1 down these columns varies the $LogD_{7.4}$ values from −0.07 to 3.18. This indicates once again that compound hydrophobicity does not appear to affect the detection of binding.

The adoption of MS as a screening tool will depend not just on the availability of instrumentation but also on the analysis time and cost per sample. By running a preliminary screen at a ligand/protein ratio of 2:1, we have demonstrated that compound hits can be confidently identified and a ranking of binding affinity determined. This could be run alongside an STD-NMR screen, although this may use considerably more protein, ligand, and time. It may be possible to reduce these factors through the use of microcoil flow probes under automation, thereby acquiring these two key orthogonal screens using a single 384-well format.

EXPERIMENTAL SECTION

Protein Production and Purification. A biologically active deletion mutant of Bcl-x_L lacking the putative COOH-terminal transmembrane region and residues Met45−Ala84 (which form a flexible loop shown to be nonessential for anti-apoptotic activity)[29]

dx.doi.org/10.1021/jm201347k | J. Med. Chem. 2012, 55, 837−851

was used in this study. Unlabeled Bcl-x_L was expressed in *Escherichia coli* BLR(DE3) using the pET24b vector (Novagen). Cells were grown in 2xYT medium at 37 °C until the absorbance at 600 nm reached 0.6−0.8. They were then induced with 0.3 mM IPTG and allowed to grow for a further 16 h at 17 °C. Cells were harvested by centrifugation and lysed with sonication, and the soluble fraction was collected via centrifugation. The recombinant protein contained a C-terminal poly histidine tag (−LEHHHHHH) to facilitate one-step purification on a nickel affinity column (Ni-NTA resin, Qiagen). Uniformly labeled ^{15}N Bcl-x_L for NMR studies was prepared using the protocol for the unlabeled expression and purification as above, except that the expression used *E. coli* strain BL21(DE3). Cells were grown in M9 minimal medium supplemented with 1 g/L ^{15}N-labeled ammonium chloride as the sole nitrogen source for uniform labeling.

Targeted Compound Library Design and Characterization. One hundred and eighty compounds based around a central phenylpyrazole scaffold were designed by John Porter at UCB Pharma, Slough, U.K., and synthesized by SAI Advantium (Hyderabad, India). Compounds were diluted from 10 mM DMSO stocks prior to use. Automated Kinetic Aqueous Solubility (AKAS) assays were performed on all compounds at concentrations between 0 and 350 μM and at pH 3, 5, 7.4, and 9. Ninety-six-well filter plates were prepared with 10 μL of 10 mM DMSO stock solutions and 190 μL of 150 mM sodium phosphate buffer. Plates were shaken for 90 min and then filtered under vacuum. One hundred microliters of filtrate was transferred to 96-well UV transparent plates and analyzed on a plate reader (Molecular Devices SpectraMax190) between 240 and 400 nm. The compound concentration in the filtrate was determined by comparing absorbance values with a calibration plot to give a solubility measurement. The calibration plot was constructed by preparing 500, 200, 50, and 10 μM samples of each compound in 80:20 MeCN/H_2O. The calibration samples were transferred to a UV transparent plate and analyzed as before using a plate reader. All solubility values were measured in duplicate. High-throughput $LogD_{7.4}$ ($HTLogD_{7.4}$) values were also measured for all compounds. A 96-deep-well plate was prepared with 40 μL of 10 mM DMSO stock compound solution per well. To each well were added 400 μL of octanol and 360 μL of 150 mM sodium phosphate buffer (pH 7.4). Plates were shaken for 90 min and centrifuged. Octanol and aqueous phases were separated and analyzed by reverse phase liquid chromatography on an Agilent 1100 LC system with UV detection using Chemstation software. The concentration of sample in each phase was determined by measuring peak areas at 254 or 280 nm. The ratio of peak areas was used to calculate $HTLogD_{7.4}$ values. All compounds were measured in duplicate with an effective range of $HTLogD_{7.4}$ values from −2 to 5. All pipetting for the AKAS and $HTLogD_{7.4}$ assays was carried out using a Perkin-Elmer MultiProbeII with WinPREP software.

Mass Spectrometry. Nano-ESI MS was performed on a Waters LCT Premier mass spectrometer equipped with a Triversa NanoMate chip-based nano-ESI source (Advion Biosciences) operating in positive ion mode with a chip nozzle voltage of 1.86 kV and a spray pressure of 0.5 psi. The operating parameters of the LCT Premier were carefully adjusted to minimize in-source dissociation. The most influential parameters and their values were as follows: aperture 1 voltage, 25 V; ion guide 1, 100 V; cone voltage, 60 V; and desolvation temperature, 20 °C. The TOF analyzer was operated in V mode and the spectrometer modified to include a Speedivalve (Edwards Ltd.) connected between the rotary pump and source pumping line, allowing manual adjustment of instrument pressures. The typical pressure settings for short experiments were a source pressure of 4.65 mbar and an analyzer pressure of 2.5×10^{-6} mbar. The spectrometer pressure used for a full screen (taking 5 h) was reduced slightly to 4.41 mbar and 1.9×10^{-6} mbar in the source/analyzer regions, respectively.

Protein samples were desalted prior to use, for large volumes by dialysis against 20 mM ammonium acetate buffer (pH 6.8) and for small volumes by Micro Bio-Spin 6 columns (Bio-Rad). For K_D determination of the lysozyme/NAG_n system, protein concentration was held at 10 μM while five titration points were taken for each ligand, where [L]$_0$ was varied to pass through the expected K_D value. Ligand stock solutions were prepared in 20 mM ammonium acetate buffer (pH 6.8). For K_D determination it was assumed that P and PL gave the same linear detector response. The peak heights for the P and PL complexes from data deconvoluted using the MaxEnt1 algorithm (Waters) were used to calculate the K_D value using eq 1, where $[L]_0$ is the initial ligand concentration.[21]

$$K_D = \frac{[P][L]}{[PL]} = \frac{[P]([L]_0 - [PL])}{[PL]} \quad (1)$$

The peak heights for P and PL were converted into concentration units by assuming that the sum of the concentrations, [P] and [PL], was equal to the initial protein concentration. The error was estimated using the standard deviation of the K_D values for each titration point.

Automated High-Throughput Screening by Mass Spectrometry. A 384-well plate was prepared with alternating rows of protein and ligand solutions using a fluid-handling robot. Protein wells contained 10 μL of a 20 μM solution, and ligand wells contained 20 μL of various concentrations from 40 to 160 μM. Two different controls with known K_D values were positioned at every 10th sample. The controls used were Bcl-x_L plus a known binder and lysozyme plus NAG_3. Plates were heat-sealed with pierceable foil covers and centrifuged (2 min, 4000 rpm). Advanced User Interface software (Advion Biosciences) was used to create an automated screening protocol with a task list as follows: pierce foil above well, aspirate 10 μL of ligand solution, dispense into a protein-containing well, aspirate and dispense for mixing (twice), aspirate 5 μL of solution, spray for 30 s into the mass spectrometer. The same sequence was repeated for each sample across the plate. Spray-sensing software (Advion Biosciences) was applied so consecutive nozzles on the NanoMate chip were used if the electrospray current dropped below 5 eV or above 400 eV for 5 s. Data acquisition was automated by connecting the NanoMate to the spectrometer via a relay switch. A sample list was created in MassLynx software (Waters) to store each spectrum in a different file for analysis. Automated deconvolution of all spectra was performed using BiopharmaLynx software (Waters), and results were taken as the relative peak heights of free protein and protein−ligand complex. An estimation of the K_D value was made with these data using eq 1 for a single value of $[L]_0$.

NMR. NMR experiments were recorded at 25 °C on a Varian VNMRS 600 MHz spectrometer equipped with a triple-resonance ^{1}H(^{13}C, ^{15}N) cryoprobe. 1D-NMR spectra were recorded for each sample to assess compound purity and protein folding. STD-NMR experiments were acquired with 512 scans according to the method described by Mayer and Meyer.[60] Selective saturation of the protein was achieved with an on-resonance irradiation frequency of −3500 Hz and off-resonance irradiation frequency of 15970.9 Hz. A train of 40 Gaussian pulses of 50 ms each with a 100 μs delay between pulses was used, with a total saturation time of 4 s. The delay between scans was 1.5 s and the sweep width, 7225 Hz. Samples for STD-NMR experiments were prepared with a protein concentration of 20 μM and ligand concentration of 1 mM in 10 mM sodium phosphate buffer, 150 mM NaCl, 100% D_2O (pH 7.3). The final volume was 200 μL in 3 mm NMR tubes. Ligands were diluted from 50 mM stock solutions in DMSO-d_6, giving 4% DMSO-d_6 (v/v) in the final sample. Control samples were prepared for each compound as above but without protein. Spectra were processed using VnmrJ (Agilent) with a line broadening of 1.5 Hz.

2D-NOESY experiments were performed on STD-NMR samples using sculpted excitation for water suppression.[61] The number of complex points in F_2 was 4308, with 64 real points in F_1. Eight scans were recorded per increment, with a total time of 40 min per experiment.

Binding Site Elucidation Using ^{1}H/^{15}N HSQC NMR Experiments. NMR data were recorded at 25 °C on a Varian VNMRS 600 MHz spectrometer equipped with a triple-resonance ^{1}H(^{13}C, ^{15}N) cryoprobe. Standard triple-resonance experiments (HNCA, HN(CO)-CA, HNCACB, CBCA(CO)NH, and HNCO) were conducted for the backbone assignment of Bcl-x_L. Uniformly ^{15}N-labeled Bcl-x_L was used at a concentration of 180 μM in 10 mM sodium phosphate buffer, 5 mM 2-mercaptoethanol (pH 7.3) with 10 % D_2O (v/v) added for a

lock signal. $^{1}H/^{15}N$ HSQC experiments were recorded on a Varian *INOVA* 600 MHz spectrometer with a room temperature probe at 25 °C. Compound was added to a final concentration of 500 μM from a 50 mM stock in DMSO-d_6 with further DMSO-d_6 added to a final 2 % (v/v) to maintain compound solubility. NMR spectra were processed with the NMRPIPE software[62] and analyzed using NMRView[63] and CcpN analysis 2.1.[64] Weighted-average chemical shift changes ($\Delta\delta_{av}$) were calculated using eq 2.[65]

$$\Delta\delta_{av} = [(\Delta\delta_H)^2 + (0.1\Delta\delta_N)^2]^{1/2} \quad (2)$$

ITC. ITC experiments were completed with both VP-ITC and AUTO iTC200 calorimeters (MicroCal) at 25 °C. All samples were thoroughly degassed in a ThermoVac apparatus (MicroCal) prior to use. Protein was dialyzed into PBS buffer (pH 6.8) and the protein dialysate used to prepare the ligand titrate. DMSO was added to each solution to a final volume of 4%. Bcl-x_L (150 μM) was placed in the reaction cell, and 2 mM ligand solution was injected using 1 × 3 μL and 24 × 6 μL injections with a 12 s interval between each. To ensure complete mixing, the reaction cell was continuously stirred at 310 rpm. The first injection was removed prior to each analysis to correct for anomalous effects due to diffusion from the syringe during equilibration. The heat due to dilution, mechanical effects, and other nonspecific effects was accounted for by averaging the last three points of the titration and subtracting that value from all data points.[66−68] Data were fitted with a single-site binding model using Origin software (MicroCal). The enthalpy change, ΔH, association constant, K_a, and binding stoichiometry, n, were not fixed during the least-squares minimization process, and the best-fit values were taken.

■ ASSOCIATED CONTENT

Supporting Information

STD-NMR spectra and ITC isotherms for the lysozyme/NAG_n interactions study given in Figure 2F. Simulated binding curves as an extension to the data provided in Figure 6. MS screening results for additional screens at increasing L/P ratios. 2D-NOESY spectra and ITC isotherms from the results summarized in Table 2. This material is available free of charge via the Internet at http://pubs.acs.org.

■ AUTHOR INFORMATION

Corresponding Author

*Phone: (M.P.C.)+44 (0)117 3317163, (J.C.)+44 (0)117 9288445. Fax: +44 (0)117 9298611. E-mail: (M.P.C.) matt.crump@bristol.ac.uk, (J.C.) john.crosby@bristol.ac.uk.

■ ACKNOWLEDGMENTS

We acknowledge Dr. Christopher Arthur and Dr. Paul Gates in the Bristol Mass Spectrometry service and Dr. Christopher Williams for assistance with high-field NMR spectroscopy. We thank UCB Pharma, Slough, U.K., and the BBSRC for the award of a BBSRC postgraduate Industrial Partnership Grant to H.J.M. (BB/E528895/1).CSP, chemical shift perturbation; FAXS, fluorine chemical shift anisotropy and exchange for screening; FBDD, fragment-based drug discovery; HSQC, heteronuclear single-quantum coherence; HTS, high-throughput screening; ITC, isothermal titration calorimetry; NAG_3, *N,N′,N″*- triacetylglucosamine; nano-ESI MS, nanoelectrospray ionization mass spectrometry; NMR, nuclear magnetic resonance; NOESY, nuclear Overhauser enhancement spectroscopy; RSD, relative standard deviation; SPR, surface plasmon resonance; STD, saturation transfer difference; UV, ultraviolet spectroscopy

■ REFERENCES

(1) Carr, R. A. E.; Congreve, M.; Murray, C. W.; Rees, D. C. Fragment-Based Lead Discovery: Leads by Design. *Drug Discovery Today* **2005**, *10*, 987−992.

(2) Whittaker, M.; Law, R. J.; Ichihara, O.; Hesterkamp, T.; Hallett, D. Fragments: Past, Present and Future. *Drug Discovery Today: Technol.* **2010**, *7*, 163−171.

(3) Howard, S.; Berdini, V.; Boulstridge, J. A.; Carr, M. G.; Cross, D. M.; Curry, J.; Devine, L. A.; Early, T. R.; Fazal, L.; Gill, A. L.; Heathcote, M.; Maman, S.; Matthews, J. E.; McMenamin, R. L.; Navarro, E. F.; O'Brien, M. A.; O'Reilly, M.; Rees, D. C.; Reule, M.; Tisi, D.; Williams, G.; Vinkovic, M.; Wyatt, P. G. Fragment-Based Discovery of the Pyrazol-4-yl Urea (AT9283), a Multitargeted Kinase Inhibitor with Potent Aurora Kinase Activity. *J. Med. Chem.* **2009**, *52*, 379−388.

(4) Murray, C. W.; Carr, M. G.; Callaghan, O.; Chessari, G.; Congreve, M.; Cowan, S.; Coyle, J. E.; Downham, R.; Figueroa, E.; Frederickson, M.; Graham, B.; McMenamin, R.; O'Brien, M. A.; Patel, S.; Phillips, T. R.; Williams, G.; Woodhead, A. J.; Woolford, A. J.-A. Fragment-Based Drug Discovery Applied to Hsp90. Discovery of Two Lead Series with High Ligand Efficiency. *J. Med. Chem.* **2010**, *53*, 5942−5955.

(5) Dalvit, C. NMR Methods in Fragment Screening: Theory and a Comparison with other Biophysical Techniques. *Drug Discovery Today* **2009**, *14*, 1051−1057.

(6) Geitmann, M.; Elinder, M.; Seeger, C.; Brandt, P.; De Esch, I. J. P.; Danielson, U. H. Identification of a Novel Scaffold for Allosteric Inhibition of Wild Type and Drug Resistant HIV-1 Reverse Transcriptase by Fragment Library Screening. *J. Med. Chem.* **2011**, *54*, 699−708.

(7) Torres, F. E.; Recht, M. I.; Coyle, J. E.; Bruce, R. H.; Williams, G. Higher Throughput Calorimetry: Opportunities, Approaches and Challenges. *Curr. Opin. Struct. Biol.* **2010**, *20*, 598−605.

(8) Jhoti, H.; Cleasby, A.; Verdonk, M.; Williams, G. Fragment-Based Screening Using X-Ray Crystallography and NMR Spectroscopy. *Curr. Opin. Chem. Biol.* **2007**, *11*, 485−493.

(9) Hofstadler, S. A.; Sannes-Lowery, K. A. Applications of ESI-MS in Drug Discovery: Interrogation of Noncovalent Complexes. *Nat. Rev. Drug. Discov.* **2006**, *5*, 585−595.

(10) Breuker, K.; McLafferty, F. W. Stepwise Evolution of Protein Native Structure with Electrospray into the Gas Phase, 10^{-12} to 10^{2} s. *Proc. Natl. Acad. Sci. U.S.A.* **2008**, *105*, 18145−18152.

(11) Benesch, J. L. P.; Robinson, C. V. Dehydrated but Unharmed. *Nature* **2009**, *462*, 576−577.

(12) Schmidt, A.; Karas, M. The Influence of Electrostatic Interactions on the Detection of Heme−Globin Complexes in ESI-MS. *J. Am. Soc. Mass Spectrom.* **2001**, *12*, 1092−1098.

(13) Yin, S.; Xie, Y.; Loo, J. A. Mass Spectrometry of Protein−Ligand Complexes: Enhanced Gas-Phase Stability of Ribonuclease−Nucleotide Complexes. *J. Am. Soc. Mass Spectrom.* **2008**, *19*, 1199−1208.

(14) Bich, C.; Baer, S.; Jecklin, M. C.; Zenobi, R. Probing the Hydrophobic Effect of Noncovalent Complexes by Mass Spectrometry. *J. Am. Soc. Mass Spectrom.* **2010**, *21*, 286−289.

(15) Liu, L.; Bagal, D.; Kitova, E. N.; Schnier, P. D.; Klassen, J. S. Hydrophobic Protein−Ligand Interactions Preserved in the Gas Phase. *J. Am. Chem. Soc.* **2009**, *131*, 15980−15981.

(16) Barylyuk, K.; Balabin, R. M.; Grünstein, D.; Kikkeri, R.; Frankevich, V.; Seeberger, P. H.; Zenobi, R. What Happens to Hydrophobic Interactions during Transfer from the Solution to the Gas Phase? The Case of Electrospray-Based Soft Ionization Methods. *J. Am. Soc. Mass Spectrom.* **2011**, *22*, 1167−1177.

(17) Freire, E. Do Enthalpy and Entropy Distinguish First in Class from Best in Class? *Drug Discovery Today* **2008**, *13*, 869−874.

(18) Robinson, C. V.; Chung, E. W.; Kragelund, B. B.; Knudsen, J.; Aplin, R. T.; Poulsen, F. M.; Dobson, C. M. Probing the Nature of Noncovalent Interactions by Mass Spectrometry. A Study of Protein-CoA Ligand Binding and Assembly. *J. Am. Chem. Soc.* **1996**, *118*, 8646−8653.

(19) Benkestock, K.; Van Pelt, C. K.; Akerud, T.; Sterling, A.; Edlund, P.-O.; Roeraade, J. Automated Nano-Electrospray Mass Spectrometry for Protein−Ligand Screening by Noncovalent Interaction Applied to Human H-FABP and A-FABP. *J. Biomol. Screen.* **2003**, *8*, 247−256.
(20) Keetch, C. A.; Hernandez, H.; Sterling, A.; Baumert, M.; Allen, M. H.; Robinson, C. V. Use of a Microchip Device Coupled with Mass Spectrometry for Ligand Screening of a Multi-Protein Target. *Anal. Chem.* **2003**, *75*, 4937−4941.
(21) Zhang, S.; Van Pelt, C. K.; Wilson, D. Quantitative Determination of Noncovalent Binding Interactions using Automated Nanoelectrospray Mass Spectrometry. *Anal. Chem.* **2003**, *75*, 3010−3018.
(22) Drinkwater, N.; Vu, H.; Lovell, K. M.; Criscione, K. R.; Collins, B. M.; Prisinzano, T. E.; Poulsen, S.-A.; McLeish, M. J.; Grunewald, G. L.; Martin, J. L. Fragment-Based Screening by X-ray Crystallography, MS and Isothermal Titration Calorimetry to Identify PNMT (Phenylethanolamine *N*-Methyltransferase) Inhibitors. *Biochem. J.* **2010**, *431*, 51−61.
(23) Hannah, V. V.; Atmanene, C.; Zeyer, D.; Van Dorsselaer, A.; Sanglier-Cianferani, S. Native MS: an 'ESI' Way to Support Structure- and Fragment-Based Drug Discovery. *Future Med. Chem.* **2010**, *2*, 35−50.
(24) Adams, J. M.; Cory, S. The Bcl-2 Protein Family: Arbiters of Cell Survival. *Science* **1998**, *281*, 1322−1326.
(25) Barelier, S.; Pons, J.; Gehring, K.; Lancelin, J.-M.; Krimm, I. Ligand Specificity in Fragment-Based Drug Design. *J. Med. Chem.* **2010**, *53*, 5256−5266.
(26) Barelier, S.; Pons, J.; Marcillat, O.; Lancelin, J.-M.; Krimm, I. Fragment-Based Deconstruction of Bcl-xL Inhibitors. *J. Med. Chem.* **2010**, *53*, 2577−2588.
(27) Hernandez, H.; Robinson, C. V. Determining the Stoichiometry and Interactions of Macromolecular assemblies from Mass Spectrometry. *Nat. Protoc.* **2007**, *2*, 715−726.
(28) Henion, J. D.; Ganem, B.; Li, Y. Observation of Noncovalent Enzyme−Substrate and Enzyme−Product Complexes by Ion-Spray Mass Spectrometry. *J. Am. Chem. Soc.* **1991**, *113*, 7818−7819.
(29) Sattler, M.; Liang, H.; Nettesheim, D.; Meadows, R. P.; Harian, J. E.; Eberstadt, M.; Yoo, H. S.; Shuker, S. B.; Chang, B. S.; Minn, A. J.; Thompson, C. B.; Fesik, S. W. Structure of Bcl-xL−Bak Peptide Complex: Recognition Between Regulators of Apoptosis. *Science* **1997**, *275*, 983−986.
(30) Benesch, J. L. P.; Ruotolo, B. T.; Simmons, D. A.; Robinson, C. V. Protein Complexes in the Gas Phase: Technology for Structural Genomics and Proteomics. *Chem. Rev.* **2007**, *107*, 3544−3567.
(31) Schultz, G. A.; Corso, T. N.; Prosser, S. J.; Zhang, S. A Fully Integrated Monolithic Microcip Electrospray Device for Mass Spectrometry. *Anal. Chem.* **2000**, *72*, 4058−4063.
(32) Liu, L.; Kitova, E. N.; Klassen, J. S. Quantifying Protein−Fatty Acid Interactions Using Electrospray Ionization Mass Spectrometry. *J. Am. Soc. Mass Spectrom.* **2011**, *22*, 310−318.
(33) Schmidt, A.; Bahr, U.; Karas, M. Influence of Pressure in the First Pumping Stage on Analyte Desolvation and Fragmentation in Nano-ESI MS. *Anal. Chem.* **2001**, *73*, 6040−6046.
(34) Tahallah, N.; Pinkse, M.; Maier, C. S.; Heck, A. J. R. The Effect of the Source Pressure on the Abundance of Ions of Noncovalent Protein Assemblies in an Electrospray Ionization Orthogonal Time-of-Flight Instrument. *Rapid Commun. Mass Spectrom.* **2001**, *15*, 596−601.
(35) Bovet, C.; Wortmann, A.; Eiler, S.; Granger, F.; Ruff, M.; Gerrits, B.; Moras, D.; Zenobi, R. Estrogen Receptor-Ligand Complexes Measured by Chip-Based Nanoelectrospray Mass Spectrometry: An Approach for the Screening of Endocrine Disruptors. *Protein Sci.* **2007**, *16*, 938−946.
(36) Veros, C. T.; Oldham, N. J. Quantitative Determination of Lysozyme−Ligand Binding in the Solution and Gas Phases by Electrospray Ionisation Mass Spectrometry. *Rapid Commun. Mass Spectrom.* **2007**, *21*, 3505−3510.
(37) Schindler, M.; Assaf, Y.; Sharon, N.; Chipman, D. M. Mechanism of Lysozyme Catalysis − Role of Ground-State Strain in Subsite-D in Hen Egg-White and Human Lysozymes. *Biochemistry* **1977**, *16*, 423−431.
(38) Imoto, T.; Johnson, L. N.; North, A. C. T.; Phillips, D. C.; Rupley, J. A. In *Vertebrate Lysozymes*, 3rd ed.; Boyer, P. D., Ed.; Academic Press: New York, 1972; pp 665−868.
(39) Porter, J.; Payne, A.; de Candole, B.; Ford, D.; Hutchinson, B.; Trevitt, G.; Turner, J.; Edwards, C.; Watkins, C.; Whitcombe, I.; Davis, J.; Stubberfield, C. Tetrahydroisoquinoline Amide Substituted Phenyl Pyrazoles as Selective Bcl-2 Inhibitors. *Bioorg. Med. Chem. Lett.* **2009**, *19*, 230−233.
(40) Lipinski, C. A.; Lombardo, F.; Dominy, B. W.; Feeney, P. J. Experimental and Computational Approaches to Estimate Solubility and Permeability in Drug Discovery and Development Settings. *Adv. Drug Delivery Rev.* **1997**, *23*, 3−25.
(41) Congreve, M.; Carr, R.; Murray, C.; Jhoti, H. A Rule of Three for Fragment-Based Lead Discovery? *Drug Discovery Today* **2003**, *8*, 876−877.
(42) Meyer, B.; Peters, T. NMR Spectroscopy Techniques for Screening and Identifying Ligand Binding to Protein Receptors. *Angew. Chem., Int. Ed.* **2003**, *42*, 864−890.
(43) Ladbury, J. E. Calorimetry as a Tool for Understanding Biomolecular Interactions and an Aid to Drug Design. *Biochem. Soc. Trans.* **2010**, *38*, 888−893.
(44) Neuhaus, D.; Williamson, M. P. In *The Nuclear Overhauser Effect in Structural and Conformational Analysis*, 2nd ed.; Marchand, A. P., Ed.; Wiley-VCH: Weinheim, Germany, 2000; pp 282−330.
(45) Davies, J. W.; Glick, M.; Jenkins, J. L. Streamlining Lead Discovery by Aligning in silico and High-Throughput Screening. *Curr. Opin. Chem. Biol.* **2006**, *10*, 343−351.
(46) Lafitte, D.; Benezech, V.; Bompart, J.; Laurent, F.; Bonnet, P. A.; Chapat, J. P.; Grassy, G.; Calas, B. Characterization of Low Affinity Complexes between Calmodulin and Pyrazine Derivatives by Electrospray Ionization Mass Spectrometry. *J. Mass. Spectrom.* **1997**, *32*, 87−93.
(47) Kitova, E. N.; Kitov, P. I.; Bundle, D. R.; Klassen, J. S. The Observation of Multivalent Complexes of Shiga-like Toxin with Globotriaoside and the Determination of Their Stoichiometry by Nanoelectrospray Fourier-Transform Ion Cyclotron Resonance Mass Spectrometry. *Glycobiology* **2001**, *11*, 605−611.
(48) Gologan, B.; Takáts, Z.; Alvarez, J.; Wiseman, J. M.; Talaty, N.; Ouyang, Z.; Cooks, R. G. Ion Soft-Landing into Liquids: Protein Identification, Separation, and Purification with Retention of Biological Activity. *J. Am. Soc. Mass Spectrom.* **2004**, *15*, 1874−1884.
(49) Strasser, A.; Huang, D. C. S.; Vaux, D. L. The Role of the Bcl-2/ced-9 Gene Family in Cancer and General Implications of Defects in Cell Death Control for Tumourigenesis and Resistance to Chemotherapy. *Biochim. Biophys. Acta* **1997**, *1333*, F151−F178.
(50) Oltersdorf, T.; Elmore, S. W.; Shoemaker, A. R.; Armstrong, R. C.; Augeri, D. J.; Belli, B. A.; Bruncko, M.; Deckwerth, T. L.; Dinges, J.; Hajduk, P. J.; Joseph, M. K.; Kitada, S.; Korsmeyer, S. J.; Kunzer, A. R.; Letai, A.; Li, C.; Mitten, M. J.; Nettesheim, D. G.; Ng, S.; Nimmer, P. M.; O'Connor, J. M.; Oleksijew, A.; Petros, A. M.; Reed, J. C.; Shen, W.; Tahir, S. K.; Thompson, C. B.; Tomaselli, K. J.; Wang, B.; Wendt, M. D.; Zhang, H.; Fesik, S. W.; Rosenberg, S. H. An Inhibitor of Bcl-2 Family Proteins Induces Regression of Solid Tumours. *Nature* **2005**, *435*, 677−681.
(51) Dennhart, N.; Letzel, T. Mass Spectrometric Real-Time Monitoring of Enzymatic Glycosidic Hydrolysis, Enzymatic Inhibition and Enzyme Complexes. *Anal. Bioanal. Chem.* **2006**, *386*, 689−698.
(52) Banerjee, S. K.; Kregar, I.; Turk, V.; Rupley, J. A. Lysozyme-Catalyzed Reaction of *N*-Acetylglucosamine Hexasaccharide − Dependance of Rate on pH. *J. Biol. Chem.* **1973**, *248*, 4786−4792.
(53) Chipman, D. M.; Sharon, N. Mechanism of Lysozyme Action. *Science* **1969**, *165*, 454−465.
(54) Dahlquist, F. W.; Jao, L.; Raftery, M. On Binding of Chitin Oligosaccharides to Lysozyme. *Proc. Natl. Acad. Sci. U.S.A.* **1966**, *56*, 26−30.

(55) Gopal, S.; Ahluwalia, J. C. Differential Scanning Calorimetric Studies on Binding of *N*-Acetyl-D-glucosamine to Lysozyme. *Biophys. Chem.* **1995**, *54*, 119−125.
(56) Rupley, J. A.; Butler, L.; Gerring, M.; Hartdege, F. J.; Pecoraro, R. Studies on the Enzymic Activity of Lysozyme, III. The Binding of Saccharides. *Proc. Natl. Acad. Sci. U.S.A.* **1967**, *57*, 1088−1095.
(57) Vulpetti, A.; Hommel, U.; Landrum, G.; Lewis, R.; Dalvit, C. Design and NMR-Based Screening of LEF, a Library of Chemical Fragments with Different Local Environment of Fluorine. *J. Am. Chem. Soc.* **2009**, *131*, 12949−59.
(58) Peschke, M.; Verkerk, U. H.; Kebarle, P. Features of the ESI Mechanism That Affect the Observation of Multiply Charged Noncovalent Protein Complexes and the Determination of the Association Constant by the Titration Method. *J. Am. Soc. Mass Spectrom.* **2004**, *15*, 1424−1434.
(59) Mathur, S.; Badertscher, M.; Scott, M.; Zenobi, R. Critical Evaluation of Mass Spectrometric Measurement of Dissociation Constants: Accuracy and Cross-Validation against Surface Plasmon Resonance and Circular Dichroism for the Calmodulin−Melittin System. *Phys. Chem. Chem. Phys.* **2007**, *9*, 6187−6198.
(60) Mayer, M.; Meyer, B. Characterization of Ligand Binding by Saturation Transfer Difference NMR Spectroscopy. *Angew. Chem., Int. Ed.* **1999**, *38*, 1784−1788.
(61) Hwang, T. L.; Shaka, A. J. Water Suppression That Works. Excitation Sculpting Using Arbitrary Wave-Forms and Pulsed-Field Gradients. *J. Magn. Reson., Ser. A* **1995**, *112*, 275−279.
(62) Delaglio, F.; Grzesiek, S.; Vuister, G. W.; Zhu, G.; Pfeifer, J.; Bax, A. NMRPIPE − A Multidimensional Spectral Processing System Based on Unix Pipes. *J. Biomol. NMR* **1995**, *6*, 277−293.
(63) Johnson, B. A.; Blevins, R. A. NMR VIEW − A Computer Program for the Visualization and Analysis of NMR Data. *J. Biomol. NMR* **1994**, *4*, 603−614.
(64) Vranken, W. F.; Boucher, W.; Stevens, T. J.; Fogh, R. H.; Pajon, A.; Llinas, M.; Ulrich, E. L.; Markley, J. L.; Ionides, J.; Laue, E. D. The CCPN Data Model for NMR Spectroscopy: Development of a Software Pipeline. *Proteins* **2005**, *59*, 687−696.
(65) Farmer, B.; Constantine, K. L.; Goldfarb, V.; Friedrichs, M. S.; Wittekind, M.; Yanchunas, J.; Robertson, J. G.; Mueller, L. Localizing the NADP(+) Binding Site on the MurB Enzyme by NMR. *Nat. Struct. Biol.* **1996**, *3*, 995−997.
(66) Kittleson, J. T.; Loftin, I. R.; Hausrath, A. C.; Engelhardt, K. P.; Rensing, C.; McEvoy, M. M. Periplasmic Metal-Resistance Protein CusF Exhibits High Affinity and Specificity for both Cu-I and Ag-I. *Biochemistry* **2006**, *45*, 11096−11102.
(67) Bagai, I.; Liu, W.; Rensing, C.; Blackburn, N. J.; McEvoy, M. M. Substrate-Linked Conformational Change in the Periplasmic Component of a Cu(I)/Ag(I) Efflux System. *J. Biol. Chem.* **2007**, *282*, 35695−35702.
(68) Leavitt, S.; Freire, E. Direct Measurement of Protein Binding Energetics by Isothermal Titration Calorimetry. *Curr. Opin. Struct. Biol.* **2001**, *11*, 560−566.